

Supplementary Information

Long-lasting, flexible, and fully bioresorbable AZ31-tungsten batteries for transient, biodegradable electronics

Gwan-Jin Ko^{a,†}, Tae-Min Jang^{a,†}, Daiha Shin^{b,†}, Heeseok Kang^{a,c,†}, Seung Min Yang^d,
Sungkeun Han^a, Rajaram Kaveti^{e,f}, Chan-Hwi Eom^a, So Jeong Choi^a, Won Bae Han^{a,g,h}, Woon-
Hong Yeo^{g,h,i,j}, Amay J. Bandodkar^{e,f}, Jiung Cho^{k,*}, and Suk-Won Hwang^{a,l,m,*}

^aKU-KIST Graduate School of Converging Science and Technology, Korea University, Seoul, 02841, Republic of Korea

^bMetropolitan Seoul Center, Korea Basic Science Institute (KBSI), Seoul, Republic of Korea

^cCenter for Advanced Biomolecular Recognition, Biomedical Research Division, Korea Institute of Science and Technology (KIST), Seoul, 02792, Republic of Korea

^dHanwha Systems Co., Ltd., Seongnam-si, Gyeonggi-do, 13524, Republic of Korea

^eDepartment of Electrical and Computer Engineering, North Carolina State University, Raleigh, NC 27606, USA

^fCenter for Advanced Self-Powered Systems of Integrated Sensors and Technologies (ASSIST), North Carolina State University, Raleigh, NC 27606, USA

^gGeorge W. Woodruff School of Mechanical Engineering, Georgia Institute of Technology, Atlanta, GA 30332, USA.

^hIEN Center for Wearable Intelligent Systems and Healthcare, Georgia Institute of Technology, Atlanta, GA 30332, USA.

ⁱ Wallace H. Coulter Department of Biomedical Engineering, Georgia Tech and Emory University School of Medicine, Atlanta, GA, 30332, USA.

^j Parker H. Petit Institute for Bioengineering and Biosciences, Institute for Materials, Institute for Robotics and Intelligent Machines, Georgia Institute of Technology, Atlanta, GA, 30332, USA.

^k Department of Materials Science and Engineering, Hongik University, Sejong, Republic of Korea.

^l Department of Integrative Energy Engineering, Korea University, Seoul 02841, Republic of Korea

^m Biomaterials Research Center, Korea Institute of Science and Technology (KIST), Seoul 02792, Republic of Korea

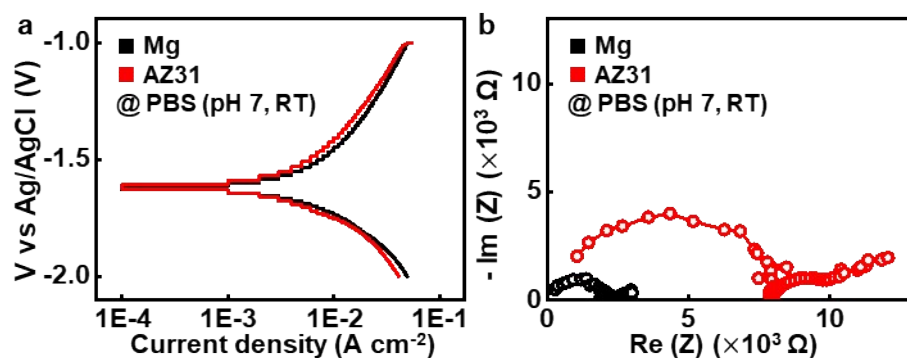


Figure S1. Comparison of electrochemical characteristics between Mg and AZ31. (a) Galvano-dynamic polarization of Mg and AZ31, showing voltage profiles corresponding to different current densities. (b) Nyquist plot of Mg and AZ31, where the diameter of the semicircle provides information about the charge transfer resistance.

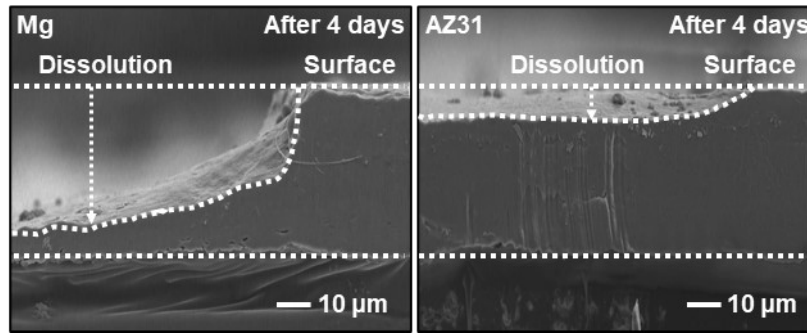


Figure S2. Cross-sectional scanning electron microscopic (SEM) images of Mg (left) and AZ31 (right) anodes, after immersion in phosphate-buffered saline (PBS, pH 7.4) solution at room temperatures for 4 days.

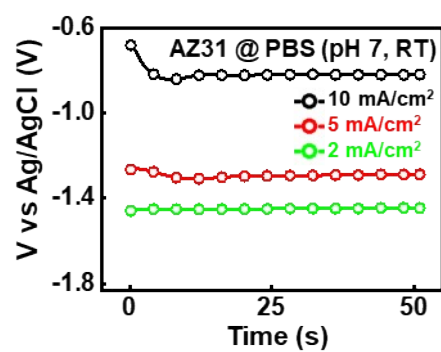


Figure S3. Measured electrodes potentials of AZ31 against the standard reference electrode (Ag/AgCl) at various discharge currents (2, 5, and 10 mA/cm²).

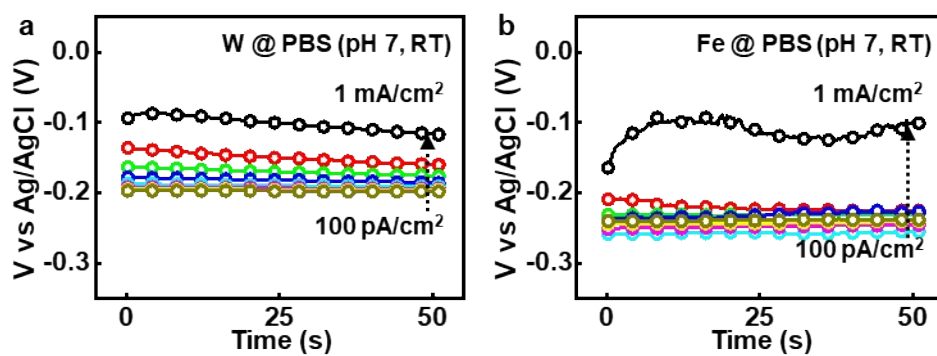


Figure S4. Temporal voltage profiles at various currents (from 100 pA/cm² to 1 mA/cm²) of W (a), and iron (b), in biological electrolyte solutions (PBS pH 7, RT). Fe showed unstable voltage outcomes when current increased due to the oxidation.

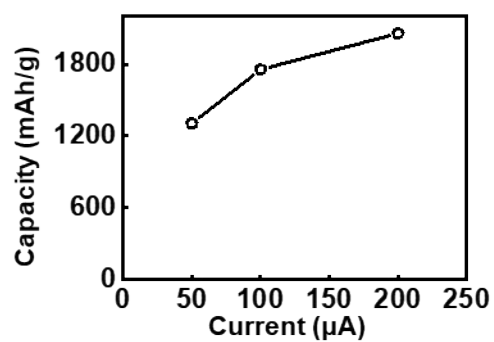


Figure S5. Capacity of an AZ31 (anode)-W (cathode) full cell in PBS solution (electrolyte) at different discharge currents.

3 parallel sets of 2 cells in series

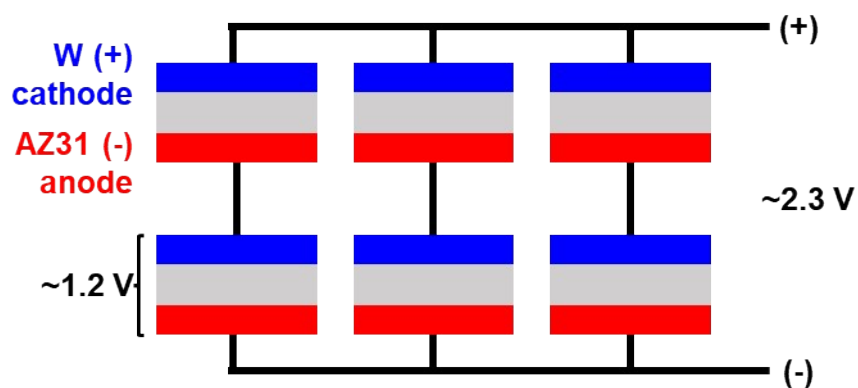


Figure S6. Circuit diagram illustrating the arrangement of W-AZ31 cells within the pouch battery.

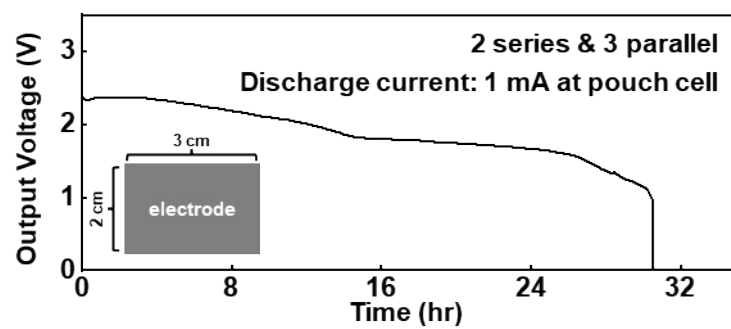


Figure S7. Discharge profiles of the pouch battery at a discharge current of 1 mA at pouch cell with the x-axis indicating discharge time.

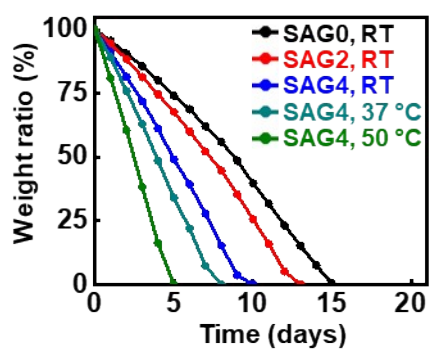


Figure S8. Time-dependent changes in weight ratios of SAG electrolyte films as a function of weight ratio of glycerol.

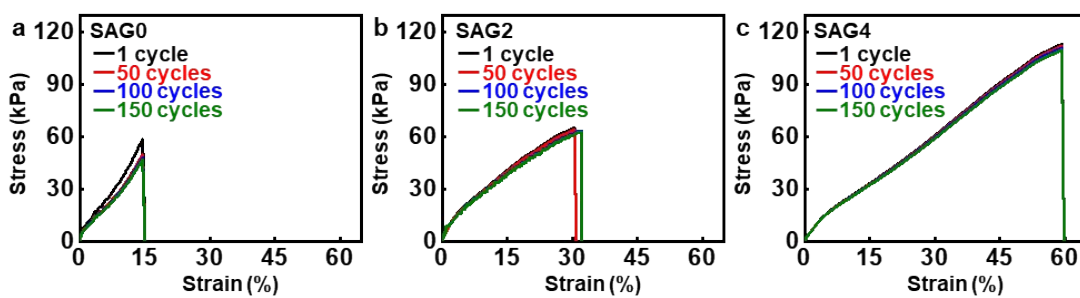


Figure S9. Mechanical cyclic stability of SAG0 (a), SAG2 (b), and SAG4 (c) electrolyte under a bend deformation at bending radius of 5 mm.

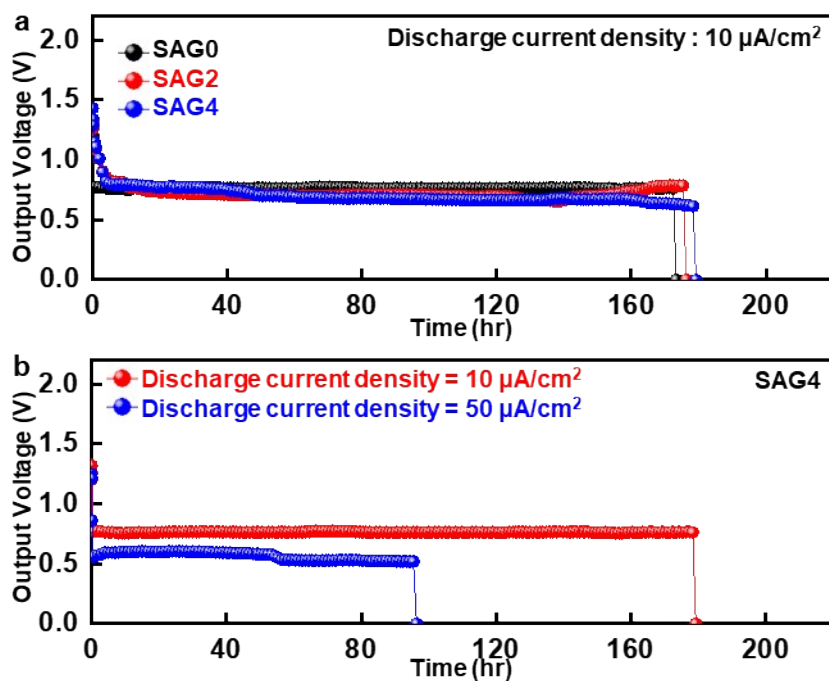


Figure S10. (a) Discharge curves of the degradable batteries based on discharge time with varying concentrations of glycerol within the solid-state electrolyte (discharge current density: 10 $\mu\text{A}/\text{cm}^2$). (b) Discharge curves of SAG4 based on discharge time with different discharge currents density.

Battery Type	Electrolyte	Working Voltage (V)	Discharge Current ($\mu\text{A}/\text{cm}^2$)	Lifetime (hr)	Ref
Mg- (Mo, W, or Fe)	PBS solution	Mo: 0.45 W: 0.65 Fe: 0.75	100	24	[1]
AZ31-PPy-pTS	Chitosan	1.33	10	160	[2]
Mg-Fe	PCL	0.7	45	99	[3]
Mg-MoO ₃	Alginate	1.6 (50hr), 0.6 (250hr)	25	312	[4]
Mg-Fe	PCL	0.45	12.5	24	[5]
Mg-Mo	Alginate	1.5	45	100	[6]
Zn-Mo	Gelatin	0.6	10	288	[7]
Zn-Mo	PLLA-PTMC	0.5	25	50	[8]
AZ31-W	Alginate	0.9	10	180	Ours

*PBS: Phosphate buffered saline

*PPy-pTS: Polypyrrole-toluene-4-sulfonic

*PCL: Polycaprolactone

*PGS: Poly (glycerol sebacate)

*PLLA-PTMC: Poly (L-lactic acid) and Poly (trimethylene carbonate)

Table S1. Comparison of previous biodegradable batteries with our approach.

References

- [1] Yin, L., Huang, X., Xu, H., Zhang, Y., Lam, J., Cheng, J., & Rogers, J. A. *Adv. Mater.* 2014, 26, 3879-3884.
- [2] X. Jia, Y. Yang, C. Wang, C. Zhao, R. Vijayaraghavan, D. R. MacFarlane, M. Forsyth and G. G. Wallace, *ACS Appl. Mater. Interfaces*, 2014, 6, 21110–21117.
- [3] Tsang, M., Armutlulu, A., Martinez, A. W., Allen, S. A. B., & Allen, M. G. *Microsystems & Nanoengineering*, 2015, 1, 1-10.
- [4] X. Huang, D. Wang, Z. Yuan, W. Xie, Y. Wu, R. Li, Y. Zhao, D. Luo, L. Cen, B. Chen, H. Wu, H. Xu, X. Sheng, M. Zhang, L. Zhao and L. Yin, *Small*, 2018, 14, 1800994.
- [5] D. She, M. Tsang and M. Allen, *Biomed. Microdevices*, 2019, 21, 17.
- [6] M. Karami-Mosammam, D. Danninger, D. Schiller and M. Kaltenbrunner, *Adv. Mater.*, 2022, 34, e2204457.
- [7] X. Huang, H. Hou, B. Yu, J. Bai, Y. Guan, L. Wang, K. Chen, X. Wang, P. Sun, Y. Deng, S. Liu, X. Cai, Y. Wang, J. Peng, X. Sheng, W. Xiong and L. Yin, *ACS Nano*, 2023, 17, 5727–5739.
- [8] B. Yu, J. Bai, Y. Guan, X. Huang, L. Liang, Z. Ren, X. Song, T. Zhang, C. Yang, F. Dai, X. Wang, X. Sheng, J. Peng, L. Wang, Y. Wang and L. Yin, *Biosens. Bioelectron.*, 2024, 263, 116578.